Regular Article

PHYSICAL CHEMISTRY RESEARCH
Published by the
Iranian Chemical Society
www.physchemres.org
info@physchemres.org

***Phys. Chem. Res.**, Vol. 6, No. 3, 493-504, September 2018*
DOI: 10.22036/pcr.2018.113197.1451

Investigation of Structural and Optoelectronic Properties of Sc_2O_3 Nanoclusters: A DFT Study

S. Hosseini, M. Vahedpour*, M. Shaterian and M.A. Rezvani

Department of Chemistry, Faculty of Science, University of Zanjan, 4537138791, Zanjan, Iran

(Received 3 January 2018, Accepted 5 May 2018)

In this manuscript, density functional theory was used to explore structural, vibrational and optical properties of the $(Sc_2O_3)_n$ (n = 1-5) cluster systems using DFT/B3LYP/LanL2DZ level of computation. Different stable isomers were obtained and numerous chemical parameters such as HOMO-LUMO gap, ionization potential and electron affinity were calculated successfully. Stability of the clusters was investigated in terms of the total and binding energies. In order to determine the origin of the species, transition states or stationary points, vibrational frequencies were calculated for the most stable configurations of $(Sc_2O_3)_n$ (n = 1-5) nanoclusters. Optical properties of scandium oxide nanoclusters were discussed using time-dependent density functional theory methods.

Keywords: Nanocluster, HOMO-LUMO gap, Vibrational frequencies, Optical properties

INTRODUCTION

Scandia has attracted particular attention for several reasons; scandium oxide has a high refractive index (n_H = 2.0 at λ = 300 nm), high band gap (5.7 eV), high ultraviolet cut-off (215 nm) and high melting point (~2485 °C) [1]. It is used as a stabilizer for highly conducing ZrO_2-based solid electrolytes, sintering aid for super-strong silicon nitride ceramics and dopant in gadolinium gallium garnet (GGG) solid-state lasers. More recently, the incorporation of Sc_2O_3 in NO_x and CO_2 sensors, and in cathodes for high-resolution/high-brightness cathode ray tubes also have been studied [2]. The prediction of the atomic structure of materials is crucial. In recent years, considerable effort has been made to understand clusters. Clusters are aggregates of atoms or molecules intermediate in size between individual atoms and bulk matter. Many interesting properties of clusters such as the optical, magnetic and mechanical characteristics change as their size varies [3]. Due to their novel physical and chemical properties and their technological applications, metal oxide clusters have a significant role in cluster physics. For example, transition metal oxide clusters usually exhibit interesting reactions with toxic gas molecules. Metal oxide clusters are useful in molecular imaging, gas sensing, information storage, catalysts, solar cells, and so on [4]. Their studies can lead to the discovery of new materials with varying properties by changing size and shape. Experimental and theoretical investigations of atomic and molecular clusters have been widely considered over the last 15 years [5]. It is difficult to obtain structural information of small nanoparticles from experiment, therefore, computational simulations have become increasingly useful for identification of physical and chemical properties of nanoclusters at the atomic level or analysis of experimental observations. The density functional theory (DFT) is a proper approach to assess the structural and electronic properties of nanoclusters which can be used to synthesize a new form of the engineering applications [6]. A literature review showed that no particular models have yet been performed to predict the electronic and spectroscopic properties of $(Sc_2O_3)_n$ (n = 1-5) [7,8].

*Corresponding author. E-mail: vahed@znu.ac

During this study, different structures of Sc_2O_3 nanocluster are designed and optimized computationally. For more stable structures, total energies, binding energies, dipole moment, density of states (DOS), HOMO-LUMO gap, ionization potential and electron affinity are also calculated using the DFT approach. The optical properties of the selected structures aaccomplished using the TD-DFT calculations as well.

COMPUTATIONAL DETAILS

All nanoclusters were optimized using the Gaussian 09 program [9]. Then, the electronic properties of optimized structures were calculated using the mentioned program package. The B3LYP method [10] in connection with the LanL2DZ basis set were used to the structural study of Sc_2O_3 nanoclusters [11]. LanL2DZ presents good results, due to the relativistic effective core potentials, ECP, in calculation of the properties of transition metal, TM, nanoclusters [12]. For visualization and analysis of frequency modes, we used VEDA 4 program [13]. DOS spectrum and HOMO-LUMO gap of Sc_2O_3 nanoclusters were obtained with Gauss sum 2.0 package [14]. The UV-Vis absorption spectra of model systems have been calculated at the TD-DFT level for all designed clusters [15].

RESULTS AND DISCUSSION

The total energy, binding energy, dipole moment, HOMO-LUMO gap, ionization potential, electron affinity, vibrational studies and optical properties for the most stable structures were investigated in this study. For finding the most stable molecules, all possible structures of Sc_2O_3 were optimized. In the next step, the relative energies per atom were calculated for all the optimized structures at the mentioned method. Then, based on the increasing the number of atoms, the structural manner for stable cluster was predicted. This manner was applied for designing the structures with upper n. Vibrational and energetic analyses were used to identify the real minimum from local minimum. The optimized geometries of all spices involved in this research were obtained in first step at the B3LYP/LanL2DZ level of calculation.

Geometrical Structures

Geometrical parameters of the stationary points are displayed in Fig. 1 and S1 of supplementary materials. The Sc_2O_3 monomer (Fig. 1a) has two Sc-O bonds that are not equal and the lengths of the bonds are 1.68 and 1.92 Å. The values of Sc-O-Sc and O-Sc-O angles are 156.4 and 116.1°, respectively. The structure of $(Sc_2O_3)_2$ is shown in Figure 1b. As seen in Fig. 1, the Sc-O bond lengths are in the range of 1.88-2.95 Å. Also, the values of O4-Sc5-O8, O8-Sc10-O9, O2-Sc6-O9 and O4-Sc10-O9 bond angles are 80.6, 83.6, 104.1 and 118.2°, respectively. The structural parameters of scandium oxide trimer, $(Sc_2O_3)_3$ are shown in Fig. 1c. The bond distances between scandium and oxygen atoms are in the range of 1.843-2.109 Å. The bond angle values of O-Sc-O in this cluster are in the range of 82.3-142.0°. The stable isomer of $(Sc_2O_3)_4$ (Fig. 1d) shows that the bond lengths between scandium and oxygen atoms are in the range of 1.864-2.206 Å, and the O-Sc-O bond angle in this cluster are in the range of 97.7-148.3°. In Fig. 1e, $(Sc_2O_3)_5$, the Sc-O bond lengths are in the range of 2.00-2.02 Å and the values of the O-Sc-O bond angles are in the range of 80.6-118°.

Bond lengths of Sc-O in the outer surface of each cluster are shorter than those in the inner layers of cluster. It may concern to the number of atomic bonds of scandium and oxygen atoms. The reverse manner is observed for the bond angles. As seen in Fig. 1, bond angles reduce in the outer surface of cluster in comparison with the inner layers. It can be attributed to the steric factor on the cluster.

The dipole moment, DP, gives the information about the arrangement of atoms and charge distributions in Sc_2O_3 nanocluster. The DP of Sc_2O_3, $(Sc_2O_3)_2$, $(Sc_2O_3)_3$, $(Sc_2O_3)_4$ and $(Sc_2O_3)_5$ clusters are 6.4, 0.0, 7.9, 0.0 and 5.8 Debye, respectively. From the results of Table 1, low dipole moments of $(Sc_2O_3)_2$ and $(Sc_2O_3)_4$ indicate that atoms are closed structure and charges present inside the nanoclusters are uniformly distributed. In contrast, the high values of dipole moment for (Sc_2O_3), $(Sc_2O_3)_3$ and $(Sc_2O_3)_5$ imply that the atoms are irregularly arranged and unequal distribution of charges have taken place in nanoclusters.

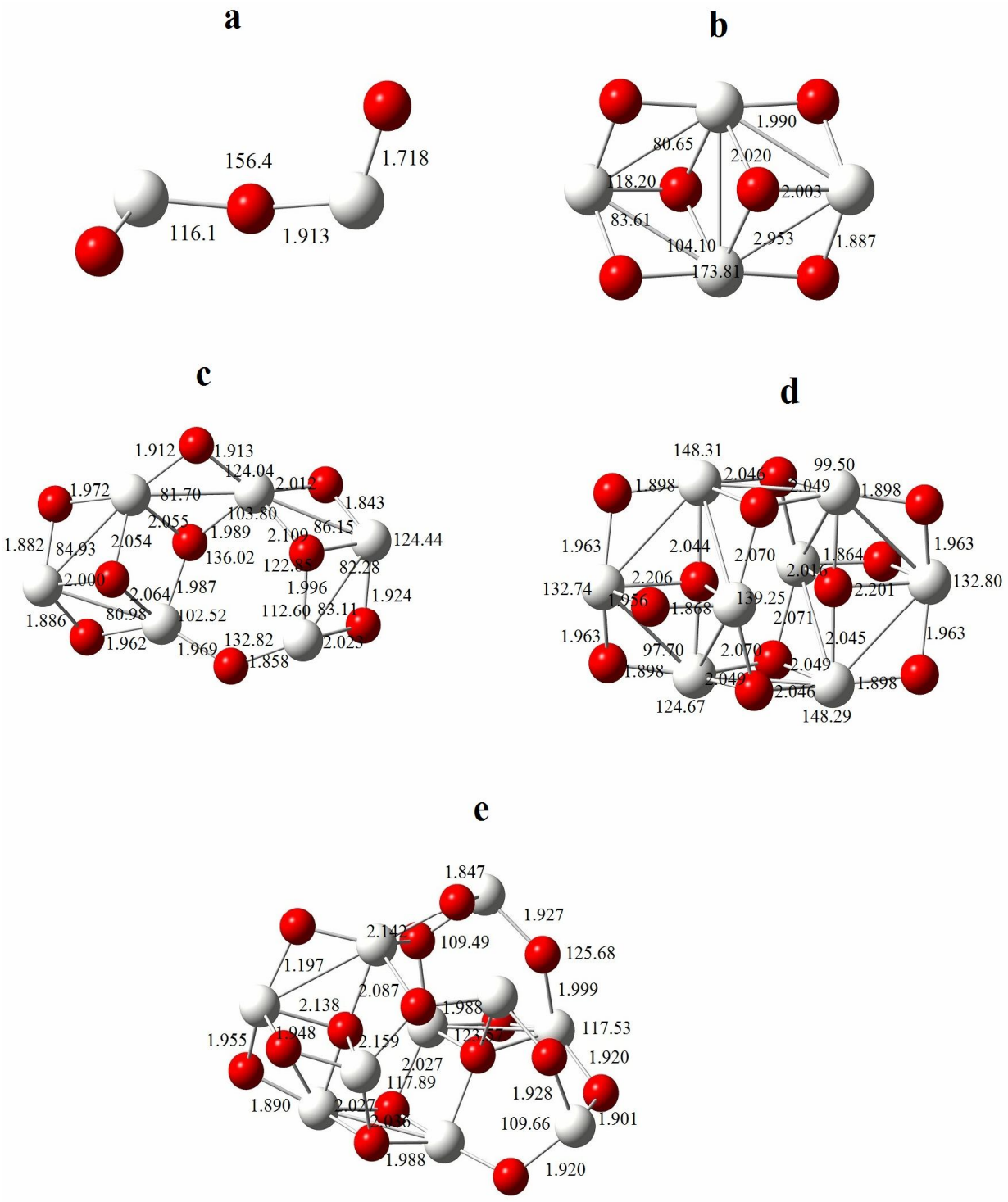

Fig. 1. B3LYP/LanL2DZ optimized geometrical parameters for the stable structures of $(Sc_2O_3)_n$ (n = 1-5). Bond lengths are given in Å and bond angles in degrees.

Table 1. Calculated Energy and Dipole Moment (DM) of $(Sc_2O_3)_n$ (n = 1-5) Nanoclusters

Entry	Calculated energy (Hartrees)	Dipole Moment (Debye)
(Sc_2O_3)	-318.7950	6.4
$(Sc_2O_3)_2$	-637.9639	0.0
$(Sc_2O_3)_3$	-957.0346	7.9
$(Sc_2O_3)_4$	-1276.1768	0.0
$(Sc_2O_3)_5$	-1595.2860	5.8

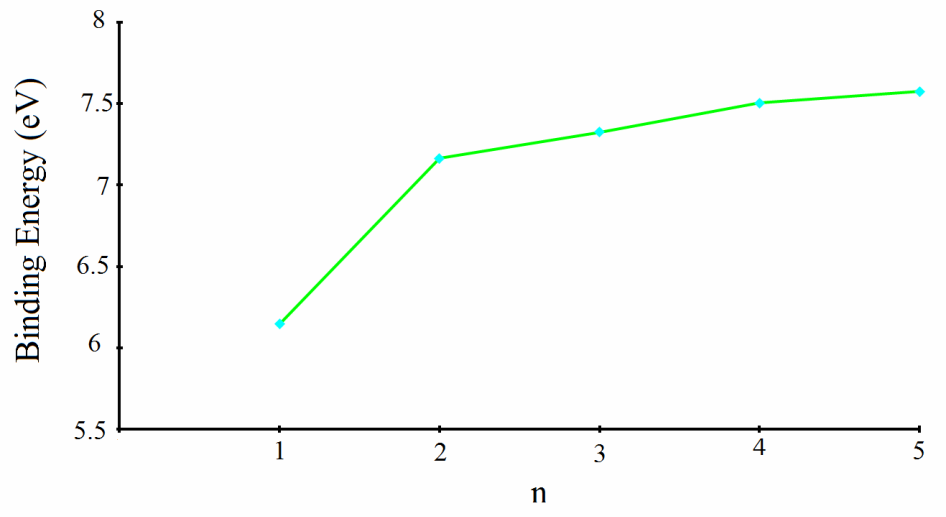

Fig. 2. Variation in binding energy per atom with n in $(Sc_2O_3)_n$ (n = 1-5) nanoclusters.

Relative Stability and Binding Energies

Binding energy is one of the important parameters to analyze the structural stability of the nanoclusters [16]. Calculated binding energy per atom (E_b) is plotted as a function of cluster size in Fig. 2. From theoretical viewpoint, this plot can be used to study the relative stability of clusters [17]. The binding energy per atom of the TM_nO_m clusters is defined as follows:

$$E_{BE} = \left(n \times E_{TM} + m \times E_O - E\left[TM_nO_m\right]\right)/\left(n+m\right) \quad (1)$$

where E_{TM} is the energy of the transition metal, E_O is the energy of oxygen, E_{TMO} is the energy of transition metal oxide and n+m is the number of transition metal and oxygen atom in the cluster. The energy of individual atoms (TM and O) is calculated separately in the same basis set, and the resultant energy values are taken into account to calculate E_{TM} and E_O [18]. Variation of total energies per atom with n in $(Sc_2O_3)_n$ nanoclusters are represented in Tables 1 and S1.

As shown in Fig. 2, the binding energy of the cluster increases with increasing the number of cluster atoms. This

property may concern to the presence of a number of cluster atoms within the cluster bulk. As known, the binding energy depends on the location of atoms. The atoms located in bulk induce more stability in the system in comparison with the atoms in cluster surface. The sharp increases (Fig. 2) at the beginning of cluster formation is related to the absence of atoms in the bulk, however, as the clusters grow, the number of bulk atoms increases and binding energy rises smoothly. The relative stability of this cluster may be due to large values of bond angles in comparison with those in the clusters with fewer monomers.

Vibrational Analysis

The normal mode vibrational analysis of the most stable structures provides further insight into the stability of the nanoclusters [19]. The optimized structures without any imaginary frequencies are named stationary points. Vibrational frequencies of the investigated nanoclusters in this study are real. All simulated vibrational frequencies and mode assignment of Sc_2O_3 nanoclusters are shown in Fig. 3 and Table S2 of supplementary materials. In Fig. 3a, the Sc_2O_3 structure has significant vibrational frequencies at 407, 840 and 956 cm^{-1} are assigned to Sc-O stretching. Lower intensity peaks within the range of 27 to 255 cm^{-1} correspond to bending and torsion vibrations of O-Sc-O, and Sc-O-Sc bond angles and O-Sc-O-Sc dihedral angle. For $(Sc_2O_3)_2$ structure (Fig. 3b), prominent intensities, 628, 682 and 733 cm^{-1}, are associated with Sc-O stretching. IR intensities of 127 and 227 km/mole are seen at the frequencies of 384 and 443 cm^{-1} that are assigned to O-Sc-O bending. The Sc-O stretching vibrational frequencies of $(Sc_2O_3)_3$ appear in 407, 493, 631, 644, 978, 660, 698, 736, 774 and 828 cm^{-1}. As seen in Fig. 3c, the Sc-O stretching modes have high absorption intensity. Frequencies at 203, 311 and 376 cm^{-1} correspond to O-Sc-O bending. Interpretation of the vibrational modes of the three-dimensional structures are very complicated. The prominent intensities for these structures are observed at frequencies in the range of 651-774 cm^{-1} with the intensities in the range of 1060.0-6032.3 km/mole. They appear due to the Sc-O stretching modes. The cluster of $(Sc_2O_3)_5$ has many vibrational modes which are observed due to arrangement of atoms in all directions (Fig. 3e). The prominent peaks are observed at frequencies in the range of 648-824 cm^{-1} which are associated with Sc-O stretching. Frequencies of 514, 312, 280, 271, 264, 252, 195, 168 and 137 cm^{-1} are arising from bending of Sc-O-Sc, O-Sc-O bond angles in $(Sc_2O_3)_5$.

Electronic Properties

Characterizing the electronic structures is of particular importance in experimental detections and some other chemical applications such as optical and magnetic properties of transition-metal oxide clusters [8]. The electronic properties of clusters are explored in terms of the energy gaps between the highest occupied molecular orbital (HOMO) and the lowest unoccupied molecular orbital (LUMO). The frontier molecule orbitals (MOs) are the most reactive MOs of a cluster. Initial interactions between the cluster and other molecules are dominated by the relative energies and the distributions of their frontier MOs. So, the frontier MOs have a close relationship with the chemical reactivity and stability of a cluster [20]. HOMO-LUMO analysis data and density of states of Sc_2O_3 nanoclusters are schematically shown in Fig. 4.

The relationship between conductivity and energy band gap (Eg) is expressed by the following equation:

$$\sigma \propto \exp\left(-\frac{Eg}{kT}\right) \tag{2}$$

here, σ is the electric conductivity and k denotes the Boltzmann constant. It is evident that a small decrease in the band gap results in significantly higher electrical conductivity [21]. As shown in Fig. 4, the HOMO-LUMO gap varies between 3.78-5.1 eV. This band gap variation demonstrates that by increasing the size of cluster, the electrical conductivity decreases and kinetic stability increases. . The largest amount of band gap value is seen for the $(Sc_2O_3)_4$ structure (Fig. 4d), due to symmetrical arrangement of Sc and O atoms and overlapping of unfilled shells in d and p orbitals of Sc and O atoms.

DOS spectrum gives detailed information about localization of charge in LUMO and HOMO levels along nanostructures [8]. Since the electronic configuration of scandium atom is $[Ar]4s^23d^1$, and oxygen is $1s^22s^22p^4$, the orbital overlapping of scandium with oxygen in a particular geometric structure gives rise to different densities of electrons in nanostructure. Moreover, by increasing the size

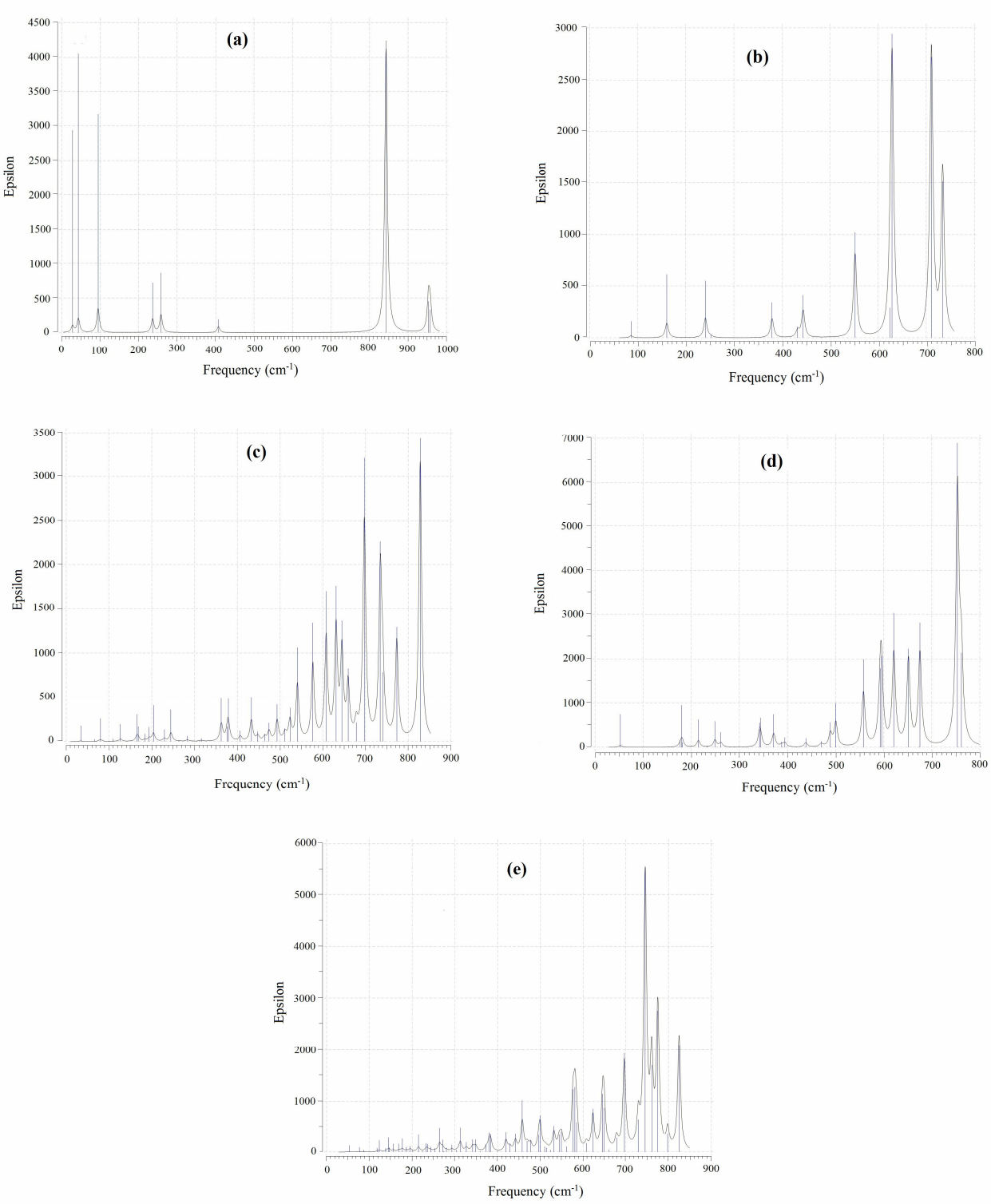

Fig. 3. Vibrational frequency and IR intensity of $(Sc_2O_3)_n$ (n = 1-5) nanoclusters. a) n = 1 b) n = 2, c) n = 3, d) n = 4, e) n = 5.

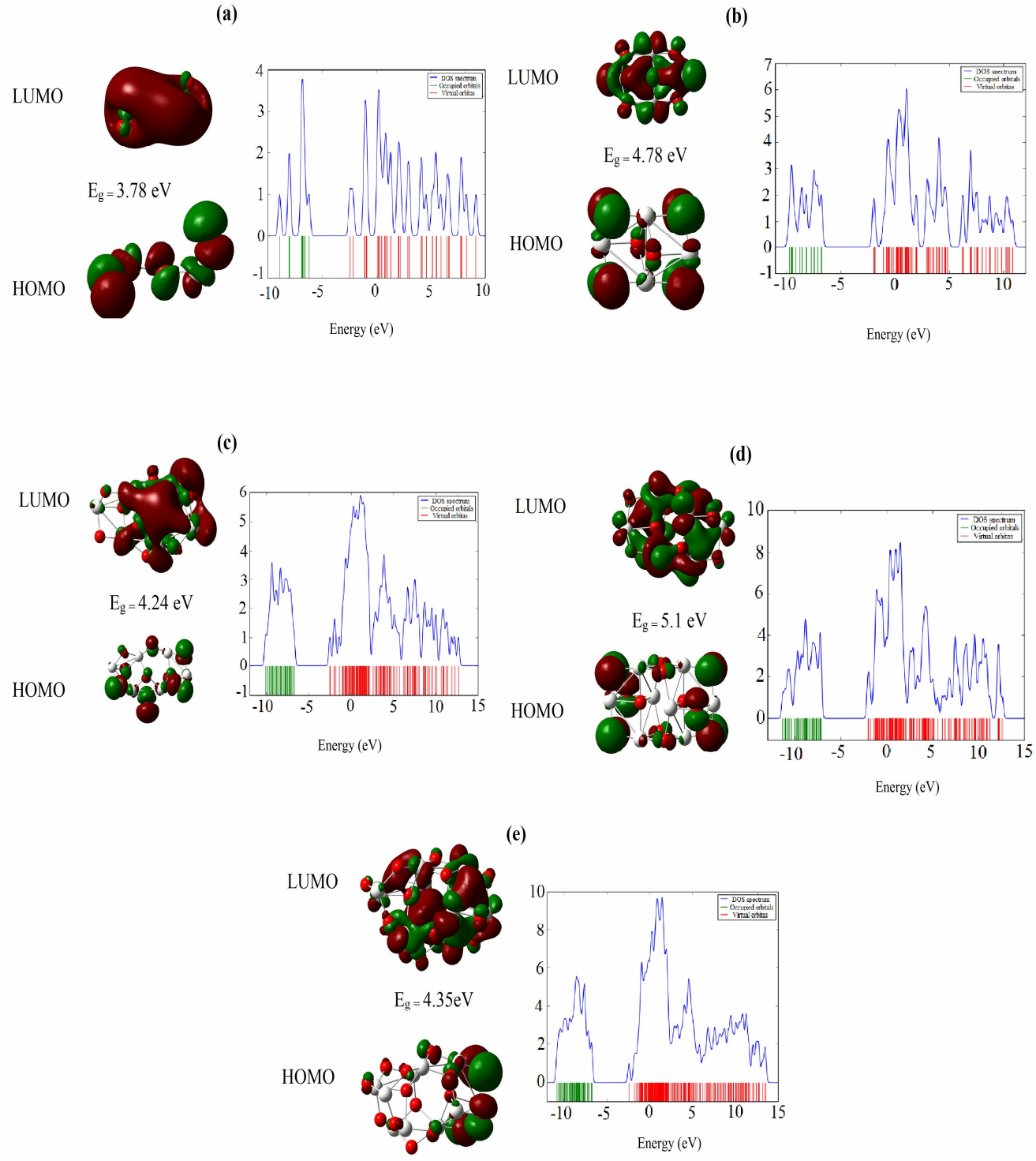

Fig. 4. HOMO-LUMO visualization and density of states of $(Sc_2O_3)_n$ (n = 1-5) nanoclusters a) n = 1 b) n = 2, c) n =3, d) n = 4, e) n = 5.

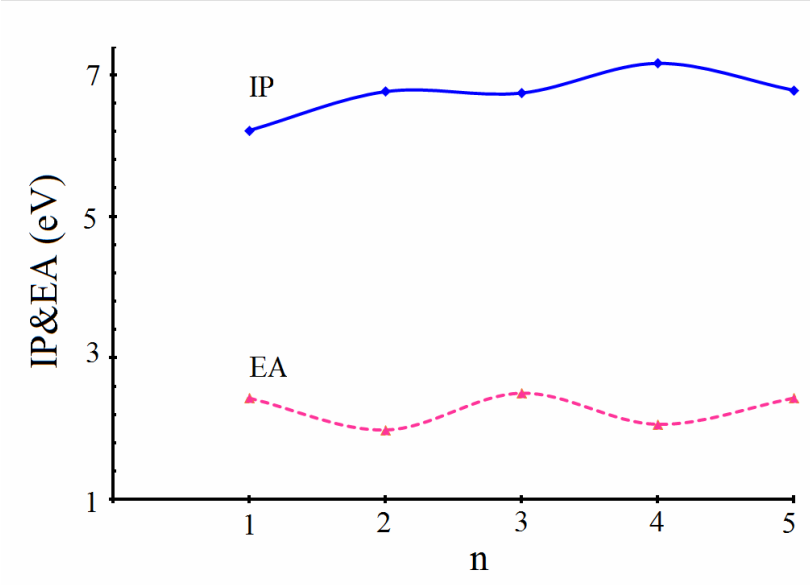

Fig. 5. EA and IP of $(Sc_2O_3)_n$ (n = 1-5) nanoclusters.

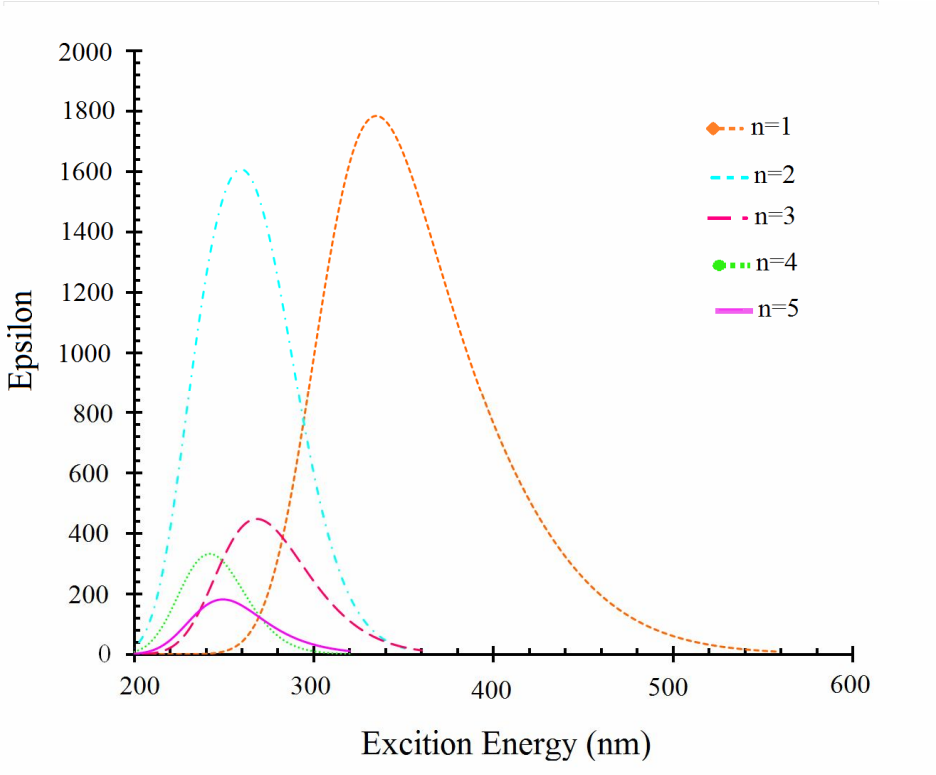

Fig. 6. The calculated TD-DFT spectra for $(Sc_2O_3)_n$ (n = 1-5) nanoclusters.

of the nanocluster structure, overlapping of scandium with oxygen in a particular geometric structure leads to amplitude of DOS peak in different energy intervals of Sc_2O_3 nanoclusters. The maximum of peak at different energy intervals arises due to the bonding of Sc and O atoms in Sc_2O_3 nanostructure. As a result, the observed maximum in virtual orbital indicates that the Sc_2O_3 nanostructure is a promising material for chemical sensor.

More and sharp HOMO peaks can cause the formation of valence band. The same manner for LUMO levels creates conduction band. Also, electron transfer from HOMO to LUMO gets easier with decreasing the Fermi level. On the other hand, when distance between conduction and valence bands (band gap) is decreased, electron transfer occurs in lower energy states. As seen in Fig. 4a, the Sc_2O_3 nanocluster shows continuous lines with lower electron transfer energy.

The electronic properties of Sc_2O_3 can be also illustrated with ionization potential (IP) and electron affinity (EA) [22]. These quantum chemical parameters were measured using Eqs. (3, 4) [23]

$$IP = -E_{HOMO} \quad (3)$$

$$EA = -E_{LUMO} \quad (4)$$

The ionization potential (IP) is the energy required to remove an electron from a nanocluster. The electron affinity (EA) refers to the energy released when an electron is added to a neutral nanocluster [23]. Figure 5 shows the variation of IP and EA of nanoclusters with cluster size. The IP values of $(Sc_2O_3)_n$, for n = 1 to 5 are 6.21, 6.76, 6.74, 7.16 and 6.78 eV, respectively. The high value of IP infers that the electrons are strongly attracted by nucleus in nanocluster. Therefore, more energy is relatively required to remove the electron from nanocluster [24] which will be more chemically inert [20].

The EA is an important parameter for the determination of chemically reactive substance as in the case of chemical sensors [25]. The calculated EA is around 1.98-2.50 eV. The high value of EA is observed for nanoclusters which are promising materials for chemical sensors owing to their high catalytic activity.

As shown in Fig. 4, the density of state diagram was merged with increasing the number of atoms in the nanocluster. This means that the virtual orbitals converged in energy and conduction band of nanocluster was formed. Similarly, the valence band was made when the occupied orbitals were forcefully joined. The difference among two bands was related to the Fermi energy, which is reported in

Optical Properties

In this subsection, the calculated TD-DFT spectra are presented for some of the structures that previously considered. TD-DFT spectra of nanoclusters are shown in Figure 6 and corresponding data including calculated maximum absorption wavelengths (λ_{max}), oscillator strengths (f), molar absorption coefficients (e_{max}) and orbital transitions are tabulated in Table 3. The major contributions with transition probabilities were greater than 10% for all the Sc_2O_3 nanoclusters.

The obtained results show that the maximum optical absorption of all the samples lies in the UV region. As a result, Sc_2O_3 nanoclusters show intense ligand-to-metal charge transfer (LMCT) absorption bands (see Table 3). Several orbitals play role in the transitions.

According to the published paper by Pari G *et al*. [26] about density-functional description of the electronic structure of metal oxides, we know that the valence band (HOMO) is comprised of 2p ($1t_{1g}$, $4t_{1u}$, $1t_{2u}$, 2_{eg}, $3a_{1g}$, $3t_{1u}$, $1t_{2g}$) orbit of O, which is in low energy, the conductive band (LUMO) is comprised of 3d (3_{eg}, $2t_{2g}$) orbit of Sc, which is near the Fermi level. The energy gap between the two bands mentioned above is also called the forbidden band or charge-transfer energy Δ_{ct}. It is found that the maximum absorption wavelengths (λ_{max}) varies in zigzag path. So, the results of this section are well matched with the results of electron characteristics.

CONCLUSIONS

The $(Sc_2O_3)_n$ nanoclusters for n = 1-5 are fully optimized at DFT-B3LYP in connection with LanL2DZ basis set. All electronic calculations are performed by the Gaussian 09 package program. The stability of the clusters was investigated in terms of the calculated total and binding energies. The stability of the clusters increases with

Table 2. TD-DFT Computed Maximum Absorption Wavelengths (λ_{max}), Oscillator Strengths (f), Molar Absorption Coefficients (e_{max}) and Orbital transitions of $(Sc_2O_3)_n$ (n = 1-5) Nanoclusters

Entry	f	λ_{max} (nm)	ε_{max} ($M^{-1}cm^{-1}$)	Major contributions (>10%)	
(Sc_2O_3)	0.0107	377.6	1779.4	HOMO (Sc 4s 21.30%, 4p 22.59%, 3d 56.12%) → LUMO (Sc 4s 4.35%, 4p 33.37%, 3d 62.29%)	(91.96)
$(Sc_2O_3)_2$	0.0201	303.2	1599.7	HOMO (O 2s 0.01%, 2p 99.99%) → LUMO (O 2s 0.01%, 2p 99.99%)	(93.30)
$(Sc_2O_3)_3$	0.0024	308.8	447.7	HOMO (Sc 4p 45.34%, 3d 54.66%) → LUMO (Sc 4s 6.92%, 4p 76.22%, 3d 16.86%)	(91.06)
$(Sc_2O_3)_4$	0.0001	286.4	322.4	HOMO (Sc 4s 0.01%, 4p 68.25%, 3d 31.74%) → LUMO (Sc 4s 0.28%, 4p 72.35%, 3d 27.37%)	(94.11)
$(Sc_2O_3)_5$	0.0002	290.4	181.9	HOMO -2 (O 2s 7.16%, 2p 92.84%) → LUMO (O 2s 5.70%, 2p 94.30%)	(91.40)

increasing the size of cluster. Frequency analysis of nanoclusters confirms that all structures are located at stationary points. The low values of dipole moments for n = 2 and 4 indicate that the atoms are in closed structure. So, distribution of the relevant nanocluster charges are uniformly. In contrast, the high values of dipole moments of n = 1, 3 and 5 imply that the arrangement of the atoms are irregular. Hence, the charge distribution in the mentioned nanoclusters is unique. In electronic transitions, as the delocalization increases, the forbidden band becomes narrower that facilitates the electron transfer from valence band (HOMO) to conductive band (LUMO), so, the semiconducting properties is higher. The results could be useful for modeling and understanding the growth of nanoclusters and providing some information about design of nanomaterials with potential optoelectronic applications.

Appendices

$$E_{BE} = \left(n \times E_{TM} + m \times E_O - E_{TM_nO_m}\right)/(n+m) \quad \text{Eq. (A.1)}$$

$$\sigma \propto \exp\left(-\frac{Eg}{kT}\right) \quad \text{Eq. (A.2)}$$

$$IP = -E_{HOMO} \quad \text{Eq. (A.3)}$$

$$EA = -E_{LUMO} \quad \text{Eq. (A.4)}$$

Abbreviations

HOMO: Highest Occupied Molecular Orbital; LUMO: Lowest Unoccupied Molecular Orbital; IP: Ionization Potential; EA: Electron Affinity; DOS: Density of states; DFT: density functional theory; TD-DFT: Time Dependent - density functional theory; DP: Dipole Moment; TM: transition metal

ACKNOWLEDGEMENTS

We gratefully acknowledge the financial supporting of University of Zanjan for this work. Also, the authors thanks from Mr Hamed Douroudgari for his help to improve of English level of paper.

REFERENCES

[1] Zhang, Y. W.; Liu, J. H.; Si, R.; Yan, Z. G.; Yan, C. H., Phase evolution, Texture behavior and surface chemistry of hydrothermally derived scandium (hydrous) oxide nanostructures. *J. Phys. Chem. B.* **2005**, *109*, 18324-18331, DOI: 10.1021/jp051870b.

[2] Li, J. G.; Ikegami, T.; Mori, T.; Yajima, Y., Sc_2O_3 Nanopowders *via* hydroxyl precipitation: Effects of sulfate ions on powder properties. *J. Am. Chem. Soc.* **2004**, *87*, 1008-1013, DOI: 10.1111/j.1551-2916.2004.01008.x.

[3] Syum, Z.; Woldeghebriel, H.; The structure and electronic properties of (GaAs)n and Al/In-doped (GaAs)n (n = 2-20) clusters. *Comput. Theor. Chem.* **2014**, *1048*, 7-17, DOI: 10.1016/j.comptc.2014.08.026.

[4] Liu, H.; Zou, X. L.; Wang, C.; Yan, J.; Duan, W., Structural transition of large lead monoxide clusters. *Comput. Theor Chem.* **2012**, *983*, 61–64, DOI: 10.1016/j.comptc.2012.01.001.

[5] Wang, H.; Hu, N.; Tao, D. J.; Lu, Zh. H.; Nie, J.; Chen, X. Sh., Structural and electronic properties of phosphorus-doped titanium clusters: A DFT study. *Comput. Theor. Chem.* **2011**, *977*, 50-54, DOI: 10.1016/j.comptc.2011.09.007.

[6] Huang, W.; Bulusu, S.; Pal, R.; Zeng, X. Ch.; Wang, L. Sh., CO chemisorption on the surfaces of the golden cages. *J. Chem. Phys.* **2009**, *131*, 23405-23410, DOI: 10.1063/1.3273326.

[7] Chertihin, G. V.; Andrews, L., Reactions of laser-ablated scandium atoms with dioxygen. infrared spectra of ScO, OScO, (O_2) ScO, $(ScO)_2$, and $Sc(O_2)_2$ in solid argon. *J. Phys. Chem. A.* **1997**, *101*, 9085-9091, DOI: 10.1021/jp972482f.

[8] Yang, Y.; Liu, H.; Zhang, P., Structural and electronic properties of ScnOm (n = 1-3, m = 1-2n) clusters: Theoretical study using screened hybrid density functional theory. *Phys. Rev. B* **2011**, *84*, 205430-205437, DOI: 10.1103/PhysRevB.84.205430.

[9] Frisch M. J., *et al*., Gaussian 03 (Revision B 03). Gaussian, Inc., Pittsburgh, PA, 2003.

[10] Chandiramouli, R.; Jeyaprakash, B. G., A DFT study on structural and electronic properties of Mn substituted CdO nanoclusters. *Eur. Phys. J. D.* **2014**, *68*, 8-16, DOI: 10.1140/epjd/e2013-40286-y.

[11] Widatallah, H. M.; Moore, E. A.; Babo, A. A.; Al-Barwani, M. S.; Elzain, M., Atomistic simulation and ab initio study of the defect structure of spinel-related Li0.50.5xMg xFe2.50.5xO4 Mater. *Res. Bull.* **2012**, *47*, 3995-4000, DOI: 10.1016/j.materresbull.2012.08.048.

[12] Balanay, M. P.; Kim, D. H., Structures and excitation energies of Zn-tetra aryl porphyrin analogues: A theoretical study. *J. Mol. Struct (THEOCHEM).* **2009**, *910*, 20-26, DOI: 10.1016/j.theochem.2009.06.010.

[13] Jamroz, M. H., Vibrational Energy Distribution Analysis VEDA 4, Warsaw, 2004-2010.

[14] O'Boyle, N. M.; Tenderholt, A. L.; Langner, K., M.m cclib: A library for package independent computational chemistry algorithms. *J. Comp. Chem.* **2008**, *29*, 839-845, DOI: 10.1002/jcc.20823.

[15] Zhai, H. J.; Li, Sh.; Dixon D. A.; Wang. L. Sh., Probing the electronic and sructural properties of chromium oxide clusters $(CrO_3)^{n-}$ and $(CrO_3)^n$ (n = 1-5): Photoelectron spectroscopy and density functional calculations, *J. Am. Chem. Soc.* **2008**, *130*, 5167-5177, DOI: 10.1021/ja077984d.

[16] Nagarajan, V.; Chandiramouli, R.; Sriram, S.; Gopinath, P., Quantum chemical studies on the structural and electronic properties of nickel sulphide and iron sulphide nanoclusters. *J. Nanostruct. Chem.* **2014**, *4*, 87-102, DOI: 10.1007/s40097-014-0087-0.

[17] Alcantar-Medina, K. O.; Herrera-Trejo, M.; Tlahuice-Flores, A.; Martinez-Vargas, S.; Oliva J.; Martinez A. I., Evolution of the structural and electronic properties of small alkali metal-doped aluminum clusters. *Comput. Theor. Chem.* **2017**, *1099*, 55-63, DOI: 10.1016/j.comptc.2016.11.008.

[18] Dwivedi, A.; Misra, N., Theoretical study of transition metal oxide clusters (TMnOm) [(TM-Pd, Rh, Ru) and (n, m = 1, 2). *J. At. Mol. Sci.* **2012**, *3*, 297-307, DOI: 10.4208/jams.092511.102611a.

[19] Yadav, P. S.; Pandey, D. K.; Agrawal, S.; Agrawal, B. K., *Ab initio* study of structural, electronic,

optical, and vibrational properties of ZnxSy (x, y = 2 to 5) nanoclusters. *J. Nanopart. Res.* **2012**, *12*, 737-757, DOI: 10.1007/s11051-010-9861-1.

[20] Ding, X. L.; Li, Z. Y.; Meng, J. H.; Zhao, Y. X.; He, S. G., Density functional global optimization of (La_2O_3)n clusters. *Chem. Phys.* **2012**, *137*, 214311-214317, DOI: 10.1063/1.4769282.

[21] Rad, A. S.; Aghaei, S. M.; Poralijan, V.; Peyravi, M.; Mirzaei, M., Application of pristine and Ni-decorated $B_{12}P_{12}$ nano-clusters as superior media for acetylene and ethylene adsorption: DFT calculations. *Comput. Theor. Chem.* **2017**, *1109*, 1-9, DOI: 10.1016/j.comptc.2017.03.030.

[22] Nagarajan, V.; Chandiramouli, R., DFT investigation on structural stability, electronic properties and CO adsorption characteristics on anatase and rutile TiO_2 nanostructures. *Ceram. Int.* **2014**, *40*, 16147-16158, DOI: 10.1016/j.ceramint.2014.07.046.

[23] Habibpour, R.; Vaziri, R., Computational study of electronic, spectroscopic, and chemical properties of $(CdO)^n$ (n = 1-7) nanoclusters as a transparent conducting oxide. *J. Part. Sci. Technol.* **2015**, *1*, 195-204, DOI: 10.22104/jpst.2015.266.

[24] Nagarajan, V.; Chandiramouli, R.; CO Adsorption characteristics on impurity substituted In_2O_3 nanostructures: A density functional theory investigation. *J. Inorg. Organomet. Polym.* **2015**, *25*, 837-847, DOI: 10.1007/s10904-015-0167-8.

[25] Zhan, C. G.; Nichols, J. A.; Dixon, D. A., Ionization potential, electron affinity, electronegativity, hardness, and electron excitation energy: Molecular properties from density functional theory orbital energies. *J. Phys. Chem. A.* **2003**, *107*, 4184-4195, DOI: 10.1021/jp0225774.

[26] Pari, G.; Jaya, S. M.; Subramoniam, G.; Asokamani, R., Density-functional description of the electronic structure of $LaMO_3$ (M = Sc, Ti, V, Cr, Mn, Fe, Co, Ni). *Phys. Rev. B. Condens. Matter.,* **1995**, *51*, 16575-16581, DOI: 10.1103/PhysRevB.51.16575.